ACS OMEGA

Open Access

http://pubs.acs.org/journal/acsodf

Article

Garbractin A, a Polycyclic Polyprenylated Acylphloroglucinol with a 4,11-dioxatricyclo[4.4.2.0^{1,5}]Dodecane Skeleton from *Garcinia bracteata* Fruits

Xue-Ni Li,⊥ Jing Xu,⊥ Shuang Yang, Qing-Qing Li, Zheng-Yang Lu, Gui Mei, Jia-Qian Li, Guang-Zhong Yang,* Xin-Xiang Lei,* and Yu Chen*

Cite This: *ACS Omega* 2023, 8, 30747−30756

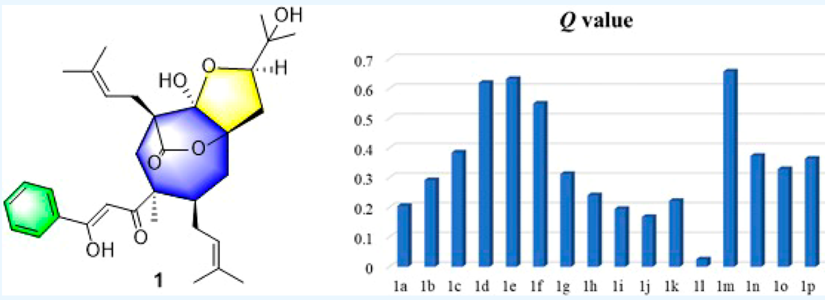

ABSTRACT: Garbractin A (**1**), a structurally complicated polycyclic polyprenylated acylphloroglucinol (PPAP) with an unprecedented 4,11-dioxatricyclo[4.4.2.0^{1,5}] dodecane skeleton, was isolated from the fruits of *Garcinia bracteata*, along with five new biosynthetic analogues named garcibracteatones A−E (**2**−**6**). Their structures containing absolute configurations were revealed using spectroscopic data, the residual dipolar coupling-enhanced NMR approach, and quantum chemical calculations. The antihyperglycemic effect of these PPAPs (**1**−**6**) was evaluated using insulin-resistant HepG2 cells (IR-HepG2 cells) induced through palmitic acid (PA). Compounds **1**, **3**, and **4** were found to significantly promote glucose consumption in the IR-HepG2 cells and, therefore, may hold potential as candidates for treating hyperglycemia.

INTRODUCTION

Polycyclic polyprenylated acylphloroglucinols (PPAPs) are a class of natural compounds that include bicyclic polyprenylated acylphloroglucinols (BPAPs), caged PPAPs, spirocyclic PPAPs, and complicated PPAPs. The complicated PPAPs with a basic tricyclo[4.3.1.0^{3,7}]decane-2,9-dione moiety such as nemorosonol and doitunggarcinone B are produced by the intramolecular [4 + 2] radical cycloaddition of monocyclic polyprenylated acylphloroglucinols (MPAPs).[1] Furthermore, the complicated PPAPs with a tricyclo[4.3.1.0^{3,7}]decane skeleton can undergo intramolecular [4 + 2] radical cycloaddition to yield the most complex PPAPs with a rare tetracyclo[4.4.1.1^{3,6}0^{9,12}]dodecane skeleton to date. Because of the novelty and intricacy of their structures, these complicated PPAPs have attracted the interest of synthetic organic chemists. The total synthesis of this class of PPAPs, including garcibracteatone and doitunggarcinone A, has been completed.[2] However, fewer than 10 cases of this class of PPAPs have been reported so far.

Previously, we reported seven new complicated PPAPs from Garcinia plants. These include garcibractinones A-B, which have a tricyclo[4.4.1.1^{1,4}]dodecane skeleton, garcibracteamones H−I and garcixanthochymones D−E, which have the rare tetracyclo-[4.4.1.1^{3,6}0^{9,12}]dodecane skeleton, and garcibracteamone J with a tricyclo[4.3.1.0^{3,7}]decane skeleton.[3] From a biosynthetic perspective, garcibractinones A−B can be traced back to the tricyclo[4.3.1.0^{3,7}]decane-2,9-dione moiety such as nemorosonol or doitunggarcinone B. It is worth noting that biosynthetic precursors for a range of structurally diverse PPAPs, including nemorosonol and doitunggarcinone B, have also been identified in the fruits of *Garcinia bracteata*. Combined with these findings, there are still new complicated PPAPs in this plant that have not yet been discovered. During our ongoing efforts to search for new complicated PPAPs from Garcinia plants, the extract of the fruits of *G. bracteata* was chemically investigated, which resulted in the isolation of six new complicated PPAPs. Garbractin A (**1**) possesses an unprecedented 4, 11-dioxatricyclo[4.4.2.0^{1,5}]-dodecane skeleton. Garcibracteatones A−E (**2**−**6**) are complicated PPAPs with a rare tetracyclo[4.4.1.1^{3,6}0^{9,12}]dodecane skeleton. The antihyperglycemic activity of these compounds

Received: July 10, 2023
Accepted: August 2, 2023
Published: August 14, 2023

https://doi.org/10.1021/acsomega.3c04947
ACS Omega 2023, 8, 30747−30756

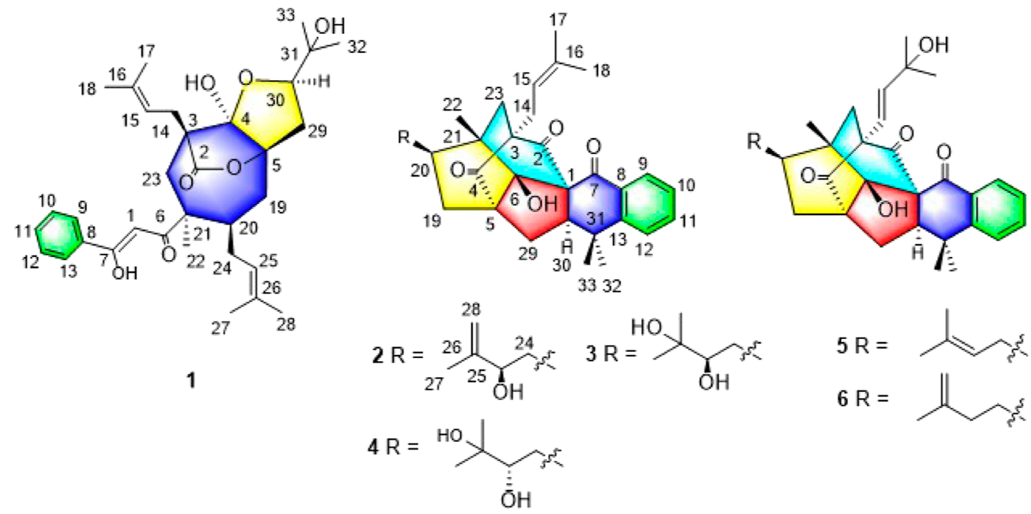

Figure 1. Structures of compounds **1**−**6**.

Table 1. ^{1}H NMR Data of Compounds **1**−**6** ($CDCl_3$, δ_H, mult, J in Hz)

position	1[a]	2[a]	3[b]	4[b]	5[b]	6[a]
1	6.11, s					
9	7.84, m	7.70, dd, (7.5, 1.0)	7.69, dd, (7.8, 1.2)	7.70, dd, (7.8, 1.2)	7.69, dd, (7.2, 1.2)	7.69, dd, (7.5, 1.5)
10	7.44, m	7.38, m	7.38, m	7.37, m	7.38, m	7.37, m
11	7.49, m	7.54, td, (7.5, 1.5)	7.55, td, (7.8, 1.2)	7.54, td, (7.8, 1.2)	7.55, td, (7.8, 1.2)	7.55, td, (8.1, 1.5)
12	7.44, m	7.36, m	7.36, m	7.37, m	7.36, m	7.36, m
13	7.84, m					
14	2.74, dd, (14.5, 9.0)	2.26, d, (7.0)	2.28, d, (7.2)	2.28, d, (7.2)	5.85, d, (16.8)	5.85, d, (16.5)
	2.38, m					
15	5.49, t, (7.5)	5.01, t, (7.5)	5.05, t, (7.2)	5.05, t, (7.2)	5.73, d, (16.2)	5.73, d, (16.0)
17	1.75, s	1.65, s	1.65, s	1.65, s	1.31, s	1.31, s
18	1.82, s	1.58, s	1.57, s	1.58, s	1.31, s	1.31, s
19	2.52, dd, (15.5, 11.5)	2.06, m	2.14, m	2.17, m	2.04, m	2.08, m
	2.05, d, (15.5)	1.73, m	1.56, m	1.84, m	1.62, m	1.63, m
20	2.20, m	1.72, m	2.22, m	2.06, m	1.94, m	1.89, m
22	1.34, s	1.45, s	1.44, s	1.49, s	1.51, s	1.50, s
23	2.25, d, (15.0)	1.81, d, (13.5)	1.78, s	1.81, d, (13.8)	2.05, m	2.05, d, (13.5)
	2.07, d, (15.0)	1.62, d, (13.5)		1.70, d, (14.4)	1.89, d, (13.8)	1.88, d, (14.0)
24	2.41, m	1.87, m	1.59, m	1.88, m	2.28, m	1.77, m
		1.73, m	1.52, m	1.44, m	2.11, m	1.52, m
25	5.05, t, (7.5)	4.07, m	3.34, d, (9.6)	3.38, d, (8.4)	5.01, dd, (7.8, 6.6)	2.05, m 1.84, m
27	1.66, s	1.71, s	1.18, s	1.17, s	1.70, s	1.72, s
28	1.73, s	4.92, br s	1.23, s	1.22, s	1.63, s	4.72, br s
		4.87, br s				4.68, br s
29	2.38, m	2.23, m	2.21, m	2.21, m	2.25, m	2.27, dd, (11.5, 10.0)
	2.19, m	2.07, m	2.10, dd, (12.0, 7.8)	2.07, m	2.10, m	2.14, dd, (11.5, 3.5)
30	3.94, dd, (8.5, 7.0)	2.66, dd, (10.0, 7.5)	2.68, dd, (9.6, 7.8)	2.67, dd, (9.6, 7.8)	2.75, dd, (10.2, 7.8)	2.76, dd, (10.0, 7.5)
32	1.10, s	1.36, s	1.36, s	1.35, s	1.37, s	1.37, s
33	1.30, s	1.09, s	1.08, s	1.08, s	1.12, s	1.11, s
4-OH	3.71, s					
6-OH		2.93, s	2.92, s	3.14, s	2.89, s	2.90, s

[a]The ^{1}H NMR spectrum was recorded at 500 MHz. [b]The ^{1}H NMR spectrum was recorded at 600 MHz.

was evaluated using insulin-resistant HepG2 cells (IR-HepG2 cells). This article reports the isolation, structural characterization, biological activity assessment, and potential biogenetic pathway of compound **1** (Figure 1).

■ RESULTS AND DISCUSSION

Compound **1** was obtained as a white, amorphous powder with a molecular formula of $C_{33}H_{44}O_7$ as inferred by a protonated molecule at m/z 553.3160 ($[M + H]^+$, calcd for $C_{33}H_{45}O_7^+$, 553.3160), indicating 12 indices of hydrogen deficiency (IHDs). The ^{1}H NMR data (Table 1) of **1** displayed the characteristic resonances of one monosubstituted benzene ring [δ_H 7.84 (2H, m); 7.44 (2H, m); 7.49 (1H, m)], seven tertiary methyls [δ_H 1.10; 1.30; 1.34; 1.66; 1.73; 1.75; 1.82 (each 3H, s)], three olefinic protons [δ_H 6.11 (1H, s); 5.49 (1H, t, J = 7.5 Hz); 5.05 (1H, t, J = 7.5 Hz)], one oxygenated methine [δ_H 3.94 (1H, dd, J

https://doi.org/10.1021/acsomega.3c04947
ACS Omega 2023, 8, 30747−30756

= 8.5, 7.0 Hz)], and a hydroxyl [δ_H 3.71 (1H, s)]. Thirty-three carbon signals were observed in the ^{13}C NMR and DEPT data (Table 2) of **1**, classified by HSQC and HMBC data as an ester carbonyl [δ_C 175.7 (s)], an enolized 1, 3-diketo moiety [δ_C 180.3 (s), 95.2 (d), 202.5 (s)], two prenyl groups [δ_C 31.1 (t), 118.4 (d), 136.5 (s), 18.5 (q), 26.5 (q); 31.5 (t), 124.7 (d), 132.6 (s), 18.3 (q), 26.1 (q)], a phenyl group [δ_C 2 × 127.1 (d), 2 × 128.7 (d), 131.9 (d), 135.3 (s)], a 2, 3-dioxygenated 3-methylbutyl group [δ_C 38.2 (t), 86.1 (d), 70.1 (s), 25.0 (q), 28.0 (q)], a hemiketal carbon [δ_C 108.8 (s)], an oxygenated tertiary carbon [δ_C 93.5 (s)]; two sp^3 quaternary carbons [δ_C 52.2 (s), 49.3 (s)], a sp^3 methine [δ_C 42.5 (d)], and two sp^3 methylenes [δ_C 35.4 (t), 44.5 (t)]. These data implied that compound **1** should be a rearranged PPAP with a tricyclic ring system.

Table 2. ^{13}C NMR Data of Compounds 1−6 (CDCl$_3$, δ_C, Type)

position	1[a]	2[a]	3[b]	4[b]	5[b]	6[a]
1	95.2, CH	69.4, C	69.3, C	69.3, C	69.3, C	69.2, C
2	175.7, C	203.0, C	203.3, C	203.4, C	202.0, C	201.9, C
3	52.2, C	63.2, C	63.3, C	63.3, C	63.7, C	63.7, C
4	108.8, C	213.3, C	213.1, C	213.4, C	212.0, C	212.0, C
5	93.5, C	70.6, C	70.3, C	70.5, C	70.5, C	70.6, C
6	202.5, C	91.9, C	92.0, C	92.1, C	91.9, C	91.8, C
7	180.3, C	200.4, C	200.6, C	200.3, C	200.2, C	200.2, C
8	135.3, C	136.6, C	136.6, C	136.5, C	136.6, C	136.5, C
9	127.1, CH	126.7, CH	126.6, CH	126.7, CH	126.6, CH	126.6, CH
10	128.7, CH	127.2, CH	127.2, CH	127.1, CH	127.2, CH	127.2, CH
11	131.9, CH	133.9, CH	133.9, CH	133.9, CH	133.9, CH	133.9, CH
12	128.7, CH	123.7, CH	123.7, CH	123.7, CH	123.7, CH	123.7, CH
13	127.1, CH	150.3, C	150.3, C	150.3, C	150.2, C	150.2, C
14	31.1, CH$_2$	25.4, CH$_2$	25.3, CH$_2$	25.3, CH$_2$	118.7, CH	118.7, CH
15	118.4, CH	118.9, CH	118.9, CH	118.9, CH	143.5, CH	143.5, CH
16	136.5, C	134.5, C	134.6, C	134.6, C	71.1, C	71.1, C
17	18.5, CH$_3$	26.0, CH$_3$	26.1, CH$_3$	26.1, CH$_3$	29.7, CH$_3$	29.7, CH$_3$
18	26.5, CH$_3$	18.1, CH$_3$	18.1, CH$_3$	18.1, CH$_3$	29.7, CH$_3$	29.6, CH$_3$
19	35.4, CH$_2$	32.8, CH$_2$	32.3, CH$_2$	33.6, CH$_2$	32.7, CH$_2$	32.7, CH$_2$
20	42.5, CH	53.6, CH	52.7, CH	55.2, CH	57.4, CH	56.7, CH
21	49.3, C	41.8, C	41.6, C	42.2, C	41.8, C	41.9, C
22	31.6, CH$_3$	19.0, CH$_3$	19.0, CH$_3$	19.1, CH$_3$	18.6, CH$_3$	18.8, CH$_3$
23	44.5, CH$_2$	47.8, CH$_2$	47.5, CH$_2$	47.8, CH$_2$	48.4, CH$_2$	48.3, CH$_2$
24	31.5, CH$_2$	39.3, CH$_2$	36.6, CH$_2$	36.1, CH$_2$	33.2, CH$_2$	32.9, CH$_2$
25	124.7, CH	75.9, CH	76.2, CH	78.8, CH	123.0, CH	36.5, CH$_2$
26	132.6, C	146.3, C	73.4, C	73.6, C	132.7, C	145.6, C
27	18.3, CH$_3$	16.5, CH$_3$	23.3, CH$_3$	23.4, CH$_3$	26.0, CH$_3$	22.6, CH$_3$
28	26.1, CH$_3$	113.5, CH$_2$	26.9, CH$_3$	26.5, CH$_3$	18.2, CH$_3$	110.5, CH$_2$
29	38.2, CH$_2$	29.2, CH$_2$	29.3, CH$_2$	29.2, CH$_2$	29.4, CH$_2$	29.4, CH$_2$
30	86.1, CH	57.0, CH	57.0, CH	57.0, CH	57.1, CH	57.1, CH
31	71.1, C	37.4, C	37.4, C	37.4, C	37.4, C	37.4, C
32	25.0, CH$_3$	26.4, CH$_3$	26.3, CH$_3$	26.5, CH$_3$	26.4, CH$_3$	26.3, CH$_3$
33	28.0, CH$_3$	30.0, CH$_3$	29.9, CH$_3$	29.8, CH$_3$	29.9, CH$_3$	29.9, CH$_3$

[a]The ^{13}C NMR spectrum was recorded at 125 MHz. [b]The ^{13}C NMR spectrum was recorded at 150 MHz.

Comprehensive analysis of the 2D NMR data revealed the presence of two substructures, A and B, in **1**. ^{1}H−^{1}H COSY spectrum (Figure 2) of H-9/H-10/H-11 together with the HMBC correlations (Figure 2) from H-9 and H-13 to δ_C 180.3 (s, C-7); HMBC correlations from H-10 and H-12 to δ_C 135.3 (s, C-8); and HMBC correlations from H-1 to δ_C 202.5 (s, C-6), 180.3 (s, C-7), and 135.3 (s, C-8) established substructure A as a 3-hydroxy-3-phenylacryloyl group. Similarly, substructure B was determined as 7-oxabicyclo-[4.2.1]nonane with a methyl connected to C-21 through ^{1}H−^{1}H COSY data of H$_2$-19/H-20/H$_2$-24/H-25, and HMBC correlations from Me-22 to δ_C 42.5 (d, C-20), 49.3 (s, C-21), and 44.5 (t, C-23); HMBC correlations from H$_2$-19 to δ_C 108.8 (s, C-4) and 93.5 (s, C-5); HMBC correlations from H$_2$-23 to δ_C 175.7 (s, C-2), 52.2 (s, C-3), and 108.8 (s, C-4), as well as the downfield chemical shift of C-13 (δ_C 93.5). Moreover, the HMBC correlations from CH$_2$-14 to δ_C 175.7 (s, C-2), 52.2 (s, C-3), 108.8 (s, C-4), and 44.5 (t, C-23); HMBC correlations from CH$_2$-19 to δ_C 31.5 (s, C-24) and δ_C 42.5 (d, C-20), HMBC correlations from Me-22 to δ_C 202.5 (s, C-6) indicated the presence of two prenyl groups and a 3-hydroxy-3-phenylacryloyl group connected to C-3, 20, and 21, respectively. The 2, 3-dioxygenated 3-methylbutyl group was attached to C-4 and C-5 and through ether linkages from C-4 to C-30 based on the key HMBC correlations from H-30 to C-4, and HMBC correlations from H$_2$-29 to C-4 and C-5. The chemical shift of C-4 at δ_C 108.8 (s) suggested the presence of a hemiketal group at C-4. Therefore, the complete planar structure of **1** was determined.

Owing to the lack of useful correlations in the ROESY data, the relative configuration of **1** was determined by NMR calculations and biosynthetic consideration. From the biosynthetic and structural analyses, compound **1** is derived from nemorosonol (Scheme 1). First, the cleavage of the C5−C6 bond by *retro*-aldol reaction led to the formation of intermediate (i). The intermediate (i) underwent further keto-enol tautomerism and *retro*-Claisen reactions to obtain the key intermediate (ii). Finally, the oxidation and esterification of intermediate (ii) could afford **1** featuring an unprecedented 4,11-dioxatricyclo[4.4.2.0^{1,5}]dodecane skeleton. According to the biosynthetic pathway, the relative configuration of C-20 and C-21 could remain unchanged, tentatively assigned as 20*R** and 21*S**, respectively. From structural analysis, compound **1** might have 16 possible diastereomers (Figure S60). To further verify the proposed conclusion, we performed NMR calculations for these 16 possible diastereomers. As a result, the corrected mean absolute deviation of 10−15 ppm and the corrected mean absolute deviation (CMAD) of 2.5−3.5 ppm were aberrantly large in those of diastereomers **1a**-**1h** with 20*R** and 21*R** configurations, which were unacceptable owing to CMAD > 2.2 ppm and CLAD >5 ppm in ^{13}C NMR calculations (Table 3).[4] Thus, it was easy to exclude the diastereomers of **1a**-**1h**. Among the remaining diastereomers, (3*R**, 4*R**, 5*R**, 20*R**, 21*S**, and 30*S**)-**1k** and (3*R**, 4*R**, 5*R**, 20*R**, 21*S**, and 30*R**)-**1l** displayed the best fit between experimental and calculated NMR shifts, indicated by the CMAD values of 1.58 and 1.67 ppm for

https://doi.org/10.1021/acsomega.3c04947
ACS Omega 2023, 8, 30747−30756

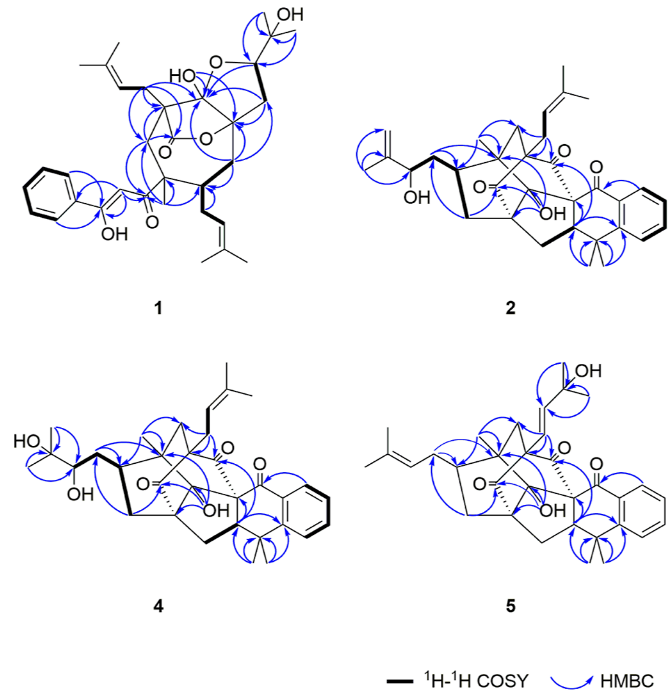

Figure 2. Key HMBC and ^{1}H−^{1}H COSY correlations of compounds **1**−**6** .

Scheme 1. Plausible Biosynthetic Pathway of Compound 1

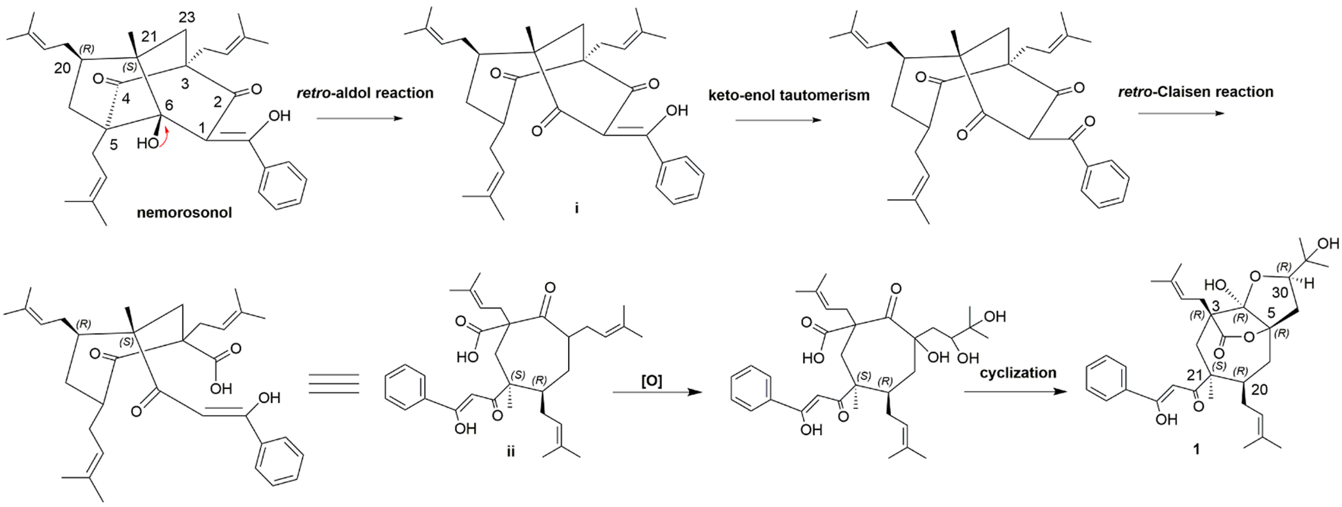

^{13}C NMR data, and 0.10 and 0.09 ppm for ^{1}H NMR data, respectively. Through these comparisons, the ^{13}C and ^{1}H NMR CMAD and RMSD for the two possible diastereoisomers **1k** and **1l** were extremely close, which made it impossible to determine whether the most likely structure for **1** was **1k** or **1l**.[5] To further identify the relative configurations of **1**, the DP4+ method for diastereomers **1i**−**1p** was employed.[6] As expected, the DP4+ method afforded 20.75 and 79.25% (Figure S62) probability for two possible diastereoisomers **1k** and **1l**, respectively. This is not an ideal value for DP4+ (preferably close to 100%), it is insufficient to consider **1l** as the most probable structure of **1**.[7]

To solve this problem, the residual dipolar coupling (RDC)-enhanced NMR method, a newly developed powerful structure resolution strategy applied for verification of the proposed molecular constitution, was employed to assign the relative configuration of **1**. RDC induced by a partial alignment of molecules in an anisotropic medium reflects rich structural information. Compared to ROE/NOE, the most widely used method in structural elucidation, which could be restricted by the distance between two protons in the space of a molecule, RDC can be employed to define the relative orientations of bonds, regardless of the distance between them. In this study, the compound was dissolved in the self-assembled AAKLVFF oligopeptide lyotropic liquid crystal, which has been developed as an alignment medium in methanol.[8] The clean and high-quality CLIP-HSQC spectra were recorded in the presence and absence of anisotropic conditions.[9] Eleven proton-carbon couplings ($^1D_{CH}$) ranging from −22.39 to 24.44 Hz were determined for analysis. Then, the configurational space of **1** was explored through molecular dynamics simulation and density functional theory (DFT) calculations. The optimized representative conformations were calculated with the B3LYP method at the 6-311G (d,p) level and Boltzmann weighted. Finally, the alignment tensor was calculated by the singular value

Table 3. Statistics of OLS-LR of Experimental and Computed ^{13}C NMR Chemical Shifts of Compound 1

compounds	CMAD[a]	CLAD[b]	R^2	RMSD[c]
rel-3*R*, 4*S*, 5*R*, 20*R*, 21*R*, 30*S*-**1a**	3.26	13.21	0.9935	4.4185
rel-3*R*, 4*S*, 5*R*, 20*R*, 21*R*, 30*R*-**1b**	3.21	15.34	0.9928	4.6516
rel-3*R*, 4*R*, 5*R*, 20*R*, 21*R*, 30*S*-**1c**	2.50	15.71	0.9948	3.9421
rel-3*R*, 4*R*, 5*R*, 20*R*, 21*R*, 30*R*-**1d**	2.65	15.8	0.9947	4.0035
rel-3*S*, 4*S*, 5*S*, 20*R*, 21*R*, 30*S*-**1e**	2.74	11.79	0.9951	3.8506
rel-3*S*, 4*S*, 5*S*, 20*R*, 21*R*, 30*R* -**1f**	2.66	12.38	0.9953	3.7588
rel-3*S*, 4*R*, 5*S*, 20*R*, 21*R*, 30*S*-**1g**	3.42	13.48	0.9932	4.5289
rel-3*S*, 4*R*, 5*S*, 20*R*, 21*R*, 30*R*-**1h**	3.18	13.6	0.9936	4.4052
rel-3*R*, 4*S*, 5*R*, 20*R*, 21*S*, 30*S*-**1i**	2.52	7.18	0.9968	3.1260
rel-3*R*, 4*S*, 5*R*, 20*R*, 21*S*, 30*R*-**1j**	2.56	7.33	0.9966	3.2221
rel-3*R*, 4*R*, 5*R*, 20*R*, 21*S*, 30*S*-**1k**	1.58	4.65	0.9987	1.9886
rel-3*R*, 4*R*, 5*R*, 20*R*, 21*S*, 30*R*-**1l**	1.67	6.42	0.9982	2.3413
rel-3*S*, 4*S*, 5*S*, 20*R*, 21*S*, 30*S*-**1m**	2.05	7.75	0.9975	2.7693
rel-3*S*, 4*S*, 5*S*, 20*R*, 21*S*, 30*R*-**1n**	2.00	8.31	0.9976	2.7117
rel-3*S*, 4*R*, 5*S*, 20*R*, 21*S*, 30*S*-**1o**	2.76	8.43	0.9956	3.6312
rel-3*S*, 4*R*, 5*S*, 20*R*, 21*S*, 30*R*-**1p**	2.75	7.77	0.9957	3.5967

[a]Corrected mean absolute deviation (CMAD). [b]Corrected mean absolute deviation (CLAD). [c]Root-mean-square deviation (RMSD).

decomposition method via the RDC module of the MSpin program.[10] Among the 16 diastereomers, (3*R**, 4*R**, 5*R**, 20*R**, 21*S**, and 30*R**)-**1l** presented the lowest *Q* factor (0.025) (Figure 3), which means that the calculated RDCs of (3*R**, 4*R**, 5*R**, 20*R**, 21*S**, and 30*R**)-**1l** have the highest degree of fitting with the experimental RDCs of **1**. Thus, the relative configuration of **1** was unequivocally determined as 3*R**, 4*R**, 5*R**, 20*R**, 21*S**, and 30*R**.

To define the absolute configuration of **1**, theoretical ECD calculations using time-dependent DFT (TDDFT) at the B3LYP/6-31+g (d,p) level were carried out. The experimental ECD spectrum of **1** had good agreement with the calculated ECD curve of (3*R*, 4*R*, 5*R*, 20*R*, 21*S*, and 30*R*)-**1l** (Figure 4). Consequently, the structure of **1** was determined as depicted in Figure 1, and it was named garbractin A.

Compound **2** was obtained as a white, amorphous powder. Its molecular formula of $C_{33}H_{40}O_5$ was inferred by a protonated molecule at m/z 517.2952 ($[M + H]^+$, calculated for $C_{33}H_{41}O_5{}^+$, 517.2949), indicating 14 IHDs. The ^1H NMR and HSQC data indicated the presence of an *ortho*-disubstituted phenyl [δ_H 7.70 (1H, dd, J = 7.5, 1.0 Hz); 7.36−738 (2H, m); 7.54 (1H, 1H, td, J = 7.5, 1.5 Hz)], six tertiary methyls [δ_H 1.09; 1.36; 1.45; 1.65; 1.58; 1.71 (each 3H, s)], three olefinic protons [δ_H 4.87 (1H, br s); 4.92 (1H, br s); 5.01 (1H, t, J = 7.5 Hz)], an oxygenated methine [δ_H 4.07 (1H, m), and a hydroxyl [δ_H 2.93 (1H, s)]. The ^{13}C NMR and DEPT data displayed a total of 33 carbon signals corresponding to three carbonyls (one conjugate and two unconjugate), six methyls, eight methines (two sp^3 carbons, one sp^3 oxygenated carbon, and five sp^2 carbons), six methylenes (five sp^3 carbons and one sp^2 carbon), and 10 nonprotonated carbons (four sp^2 quaternary carbons, one sp^3 oxygenated tertiary carbon, and five sp^3 quaternary carbons). These observations indicated **2** to be a complicated PPAP with the rare tetracyclo[4.4.1.1^{3,6}0^{9,12}] dodecane skeleton.[11,12]

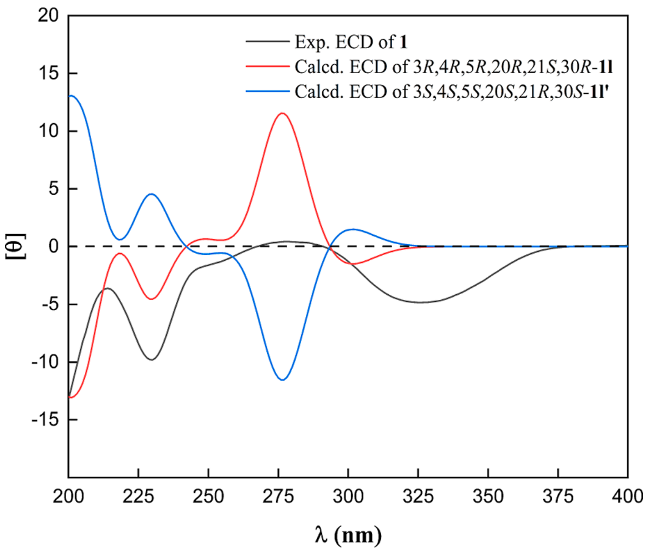

Figure 4. Experimental ECD and calculated ECD spectra of compound **1**.

Upon comparison of the NMR data of compound **2** with those of doitunggarcinone A, it was observed that the major difference was the existence of an oxygenated methine [δ_H 4.07 (m), δ_C 75.9 (d)] in compound **2**, instead of a methylene in doitunggarcinone A.[12] The results indicated that compound **2** may be a 25-hydroxy derivative of doitunggarcinone A. This deduction was further confirmed by the downfield chemical shift of C-25 (δ_C 75.9), $^1H-^1H$ COSY correlation of H_2-24/H-25, and HMBC correlations from CH_3-27 to δ_C 75.9 (d, C-25),

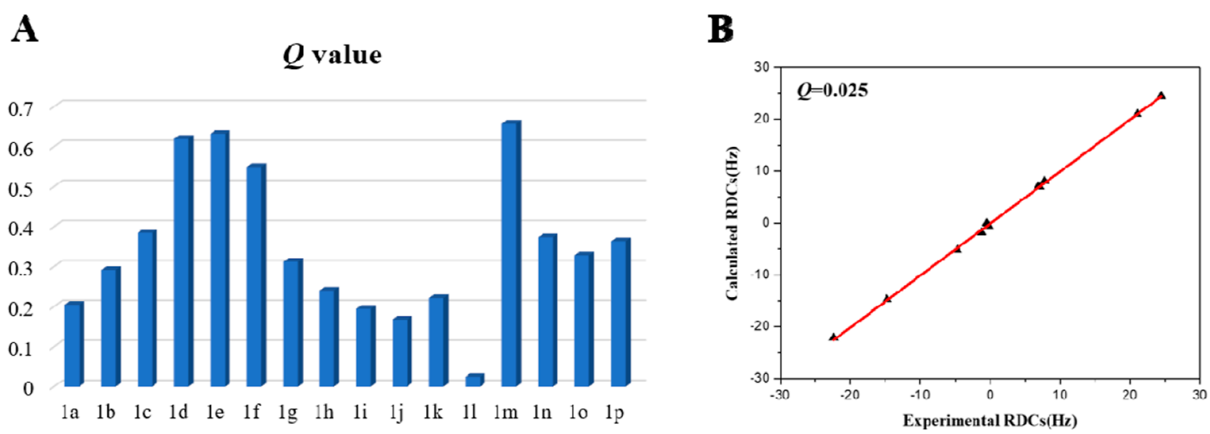

Figure 3. (A) *Q* values for 16 diastereomers fitted with experimental RDCs. (B) Correlations between the experimental and calculated $^1D_{CH}$ values of (*rel*-3*R*, 4*R*, 5*R*, 20*R*, 21*S*, and 30*R*)-**1l** .

https://doi.org/10.1021/acsomega.3c04947
ACS Omega 2023, 8, 30747−30756

146.3 (s, C-26), and 113.5 (t, C-28). Based on biosynthetic analysis, the relative configuration of **2**, with the exception of C-25, was found to be identical to that of doitunggarcinone A. This deduction was further confirmed by ROESY correlations (Figure 5) of 6-OH/CH_3−33 (δ_H 1.09), 6-OH/CH_3−22,

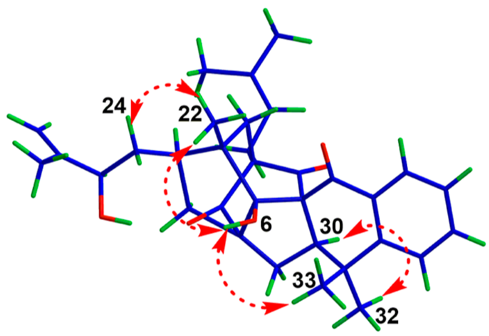

Figure 5. ROESY correlations of compound **2**.

CH_3−22/H_2−24, and H-30/CH_3−32 (δ_H 1.36). To define the configuration of C-25 in the flexible bond, NMR calculations were conducted on two possible diastereoisomers (Figure S61, 25*S**-**2a** and 25*R**-**2b**).[13] The DP4+ analysis indicated that (1*S**, 3*S**, 5*R**, 6*S**, 20*R**, 21*R**, 25*S**, and 30*S**)-**2a** was the most likely structure for **2** with a high probability of 100%. A comparison of the ECD spectrum of compound **2** with those of hyphenrones B, R, and S revealed that the ECD curves of compound **2** were just opposite to those of hyphenrones B, R, and S, indicating that the absolute configuration of compound **2** was opposite to hyphenrones B, R, and S, except for C-25.[14] This conclusion was further confirmed by ECD calculations through the TDDFT method (Figure 6). Thus, the absolute configuration of **2** was determined as (1*R*, 3*R*, 5*S*, 6*R*, 20*S*, 21*S*, 25*R*, and 30*R*).

Compounds **3** and **4** were obtained as white, amorphous powders and were found to have the same molecular formula of $C_{33}H_{42}O_6$. This was confirmed through a sodium adduct ion at *m*/*z* 557.2873 in **3** ($[M + Na]^+$, calcd for $C_{33}H_{42}O_6Na^+$, 557.2874) and a protonated molecule at *m*/*z* 535.3054 in **4** ($[M + H]^+$, calcd for $C_{33}H_{43}O_6^+$, 535.3054). A comparison of the

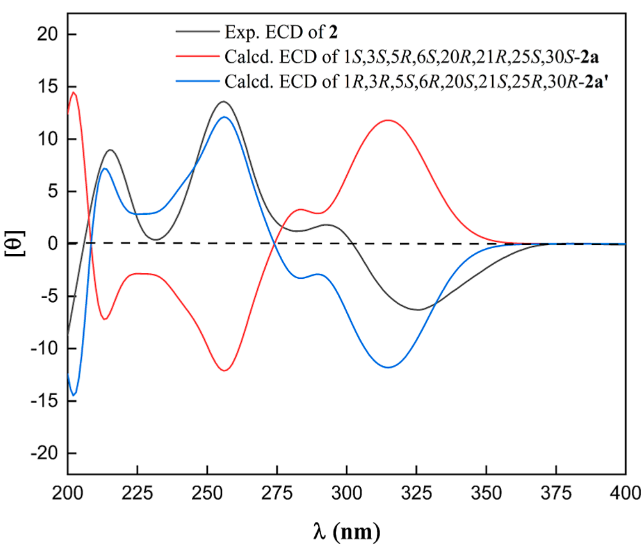

Figure 6. Experimental ECD and calculated ECD data of compound **2**.

NMR data of **3** and **4** with those of garcibracteatone revealed the presence of an oxygenated tertiary carbon and oxygenated methine in compounds **3** and **4**, instead of a trisubstituted double bond $\Delta^{25(26)}$ in garcibracteatone.[11] These findings indicated that compounds **3** and **4** may be the $\Delta^{25(26)}$-hydrate of garcibracteatone. This deduction was further confirmed by HMBC correlations from CH_3-27 and CH_3-28 to C-25 and C-26. The relative configurations of **3** and **4**, except for C-25, were found to be the same as that of compound **2** through the ROESY spectrum. To determine the absolute configurations of C-25 of the 1, 2-diol moiety in compounds **3** and **4**, we used the $Mo_2(OAc)_4$-induced circular dichroism (ICD) method. The ICD spectrum (Figure 7) of compound **3** displayed negative signs of band II at around 310 nm, while the ICD spectrum of **4** showed a positive sign of band II.[15] These results led us to assign the absolute configurations of C-25 as *R* and *S* in compounds **3** and **4**, respectively, which were consistent with the ^{13}C NMR data analysis.[16]

Compounds **5** and **6** were isolated as white, amorphous powders. Their molecular formulas of $C_{33}H_{40}O_5$ were determined by a protonated molecule at *m*/*z* 517.2951 in **5** ($[M + H]^+$, calcd for $C_{33}H_{41}O_5^+$, 517.2949) and a sodium adduct ion at *m*/*z* 539.2768 in **6** ($[M + Na]^+$, calcd for $C_{33}H_{40}O_5Na^+$, 539.2768), suggesting that compounds **5** and **6** are isomers. Comparison of the NMR data of compounds **5** and **6** with those of garcibracteatone and doitunggarcinone A revealed that compounds **5** and **6** contain (*E*)-3-hydroxy-3-methylbut-1-en-1-yl groups at C-3, instead of a prenyl group at C-3 in garcibracteatone and doitunggarcinone, respectively. This was further confirmed by the HMBC correlations from H-14 and H-15 to C-3,[11,12] and the configuration of the double bond $\Delta^{24(25)}$ was assigned the *E* on the basis of the coupling constant value of 16.2 Hz between H-14 and H-15.[17] The relative configurations of **5** and **6** were also assigned as the same as those of compounds **2**−**4** based on the ROESY spectrum.

Compounds **2**−**6** possess a fused hexacyclic system and are considered the most complex PPAPs discovered to date. These compounds are believed to be derived from tetraprenylated MPAPs, such as weddellianone A, through a sequence of intramolecular [4 + 2] radical cycloadditions, ultimately producing nemorosonol and doitunggarcinone B. These compounds then undergo a series of oxidation reactions to yield compounds **2**−**6**. Based on the analysis of the biosynthetic pathway, it is expected that the absolute configurations of compounds **2**−**6** are consistent. The absolute configuration of compound **2** was established through ECD calculations. The experimental ECD curves of compounds **3**−**6** are in good agreement with those of compound **2** (Figure 8), indicating that the absolute configurations of compounds **3**−**6**, except for C-25, are the same as that of compound **2**. Compared with compounds **2**−**4**, compounds **5** and **6** have different substituents at C-3 and C-20. According to the Cahn−Ingold−Perlog sequence rule, the configurations of C-3 and C-20 are changed to *S* and *R*, respectively.

In this study, we investigated the effects of these PPAPs on glucose consumption in IR-HepG2 cells. First, the cytotoxicity of the PPAPs to normal HepG2 cells was assessed using the CCK-8 method. The cell viabilities of compounds **1**−**6** at concentrations of 5, 10, 15, and 20 μM are shown in Table 4. Results indicated that all six compounds showed no cytotoxicity (cell viability >90%) at a concentration of 5 μM.

As depicted in Figure 9, compounds **1**, **3**, and **4** exhibited a significant increase in glucose consumption values at concen-

https://doi.org/10.1021/acsomega.3c04947
ACS Omega 2023, 8, 30747−30756

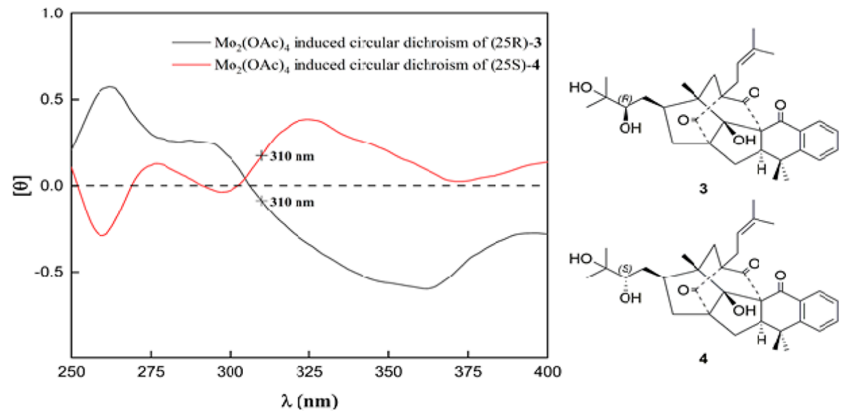

Figure 7. $Mo_2(OAc)_4$-induced ECD spectra of compounds **3** and **4** in DMSO.

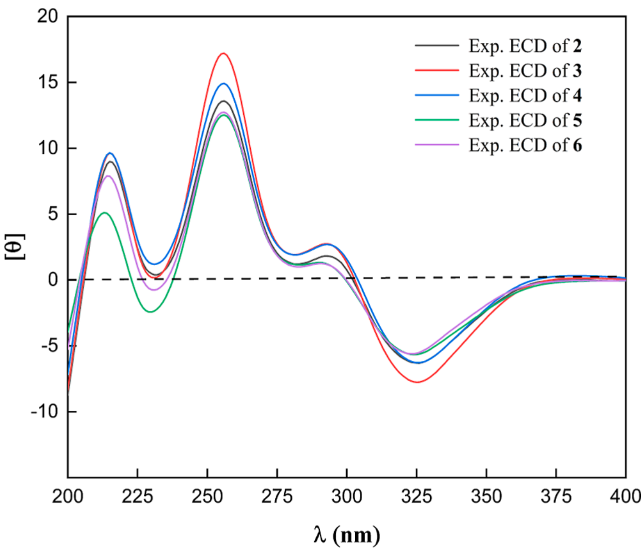

Figure 8. Experimental ECD spectra of compounds **2**−**6**.

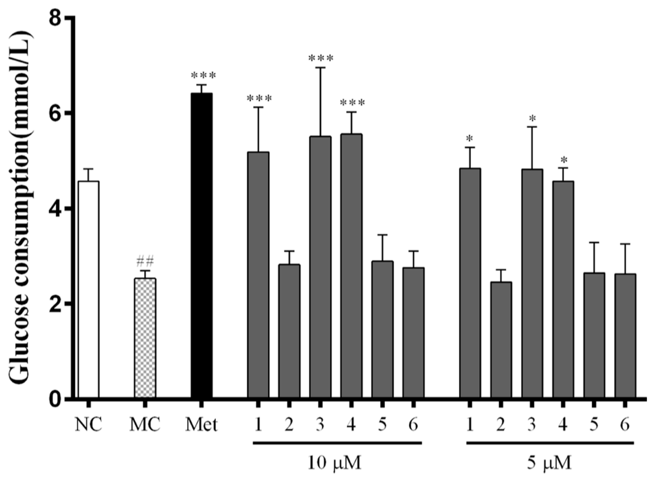

Figure 9. Effects of compounds **1**−**6** on glucose consumption in IR-HepG2 cells at concentrations of 5 and 10 μM [NC: the normal group (normal HepG2 cells); MC: the model group (IR-HepG2 cells); Met: metformin; ##$P < 0.01$ vs NC group; and *$P < 0.05$, ***$P < 0.001$ vs MC group].

trations of 5 and 10 μM compared to the IR-HepG2 model. Furthermore, at lower concentrations of 2, 4, and 6 μM, compounds **1**, **3**, and **4** exhibited a dose-dependent evaluation of glucose consumption values, as shown in Figure 10. Compounds **2**−**6** share the same carbon skeleton. The introduction of two hydroxyl groups at C-25 and C-26 of the prenyl group can enhance the biological activity of these compounds, as seen in compounds **3** and **4**. The presence of the OH group on the moiety attached to C-26 in compounds **3** and **4** may play a crucial role in the observed activity. However, the configuration of the second OH at C-25 does not seem to be significant since both compounds **3** and **4** exhibit activity. These findings indicate that the compounds **1**, **3**, and **4** possess antihyperglycemic activity. The detailed mechanism of the antihyperglycemic effects of these compounds in vivo will be explored in our future studies.

In this study, six new complicated PPAPs were isolated from the fruits of *G. bracteata*. Garbractin A (**1**) has a unique 4,11-dioxatricyclo[$4.4.2.0^{1,5}$]dodecane skeleton, while the others, garcibracteatones A−E (**2**−**6**) have a rare tetracyclo-[$4.4.1.1^{3,6}0^{9,12}$]dodecane skeleton. The biosynthetic analysis revealed that all six compounds were derived from nemorosonol or doitunggarcinon B. These findings suggest that more PPAPs

Table 4. Effect of PPAPs 1−6 on the Cell Viability of HepG2 Cells

	cell viability				
compounds	0 μM	5 μM	10 μM	15 μM	20 μM
1	100%	90.51 ± 0.18%	86.82 ± 0.16%	85.17 ± 0.18%	72.44 ± 0.19%[c]
2	100%	98.91 ± 1.60%	83.04 ± 1.24%	71.46 ± 3.32%[c]	25.61 ± 3.25%[c]
3	100%	91.47 ± 0.18%	89.30 ± 0.32%	78.29 ± 0.21%[b]	73.89 ± 0.20%[c]
4	100%	92.81 ± 0.30%	88.53 ± 0.19%	80.22 ± 0.11%[a]	76.66 ± 0.19%[b]
5	100%	99.84 ± 0.17%	78.84 ± 0.12%[b]	29.72 ± 0.14%[c]	13.43 ± 0.13%[c]
6	100%	96.33 ± 0.12%	90.28 ± 0.16%	88.50 ± 0.18%	86.56 ± 0.14%

[a]$P < 0.05$. [b]$P < 0.01$. [c]$P < 0.001$ versus 0 μM treated group.

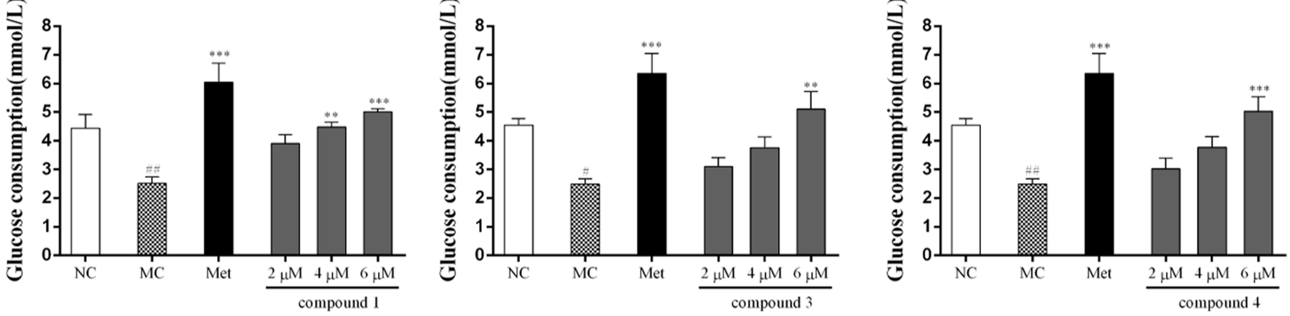

Figure 10. Effects of compounds **1**, **3**, and **4** on glucose consumption in IR-HepG2 cells at concentrations of 2, 4, and 6 μM [NC: the normal group (normal HepG2 cells); MC: the model group (IR-HepG2 cells); Met: metformin; $^{\#}P < 0.05$, $^{\#\#}P < 0.01$ vs NC group; and $^{**}P < 0.01$, $^{***}P < 0.001$ vs MC group].

with novel skeletons could be discovered from *G. bracteata* in the future. The antihyperglycemic effect of PPAPs (**1**−**6**) was evaluated using insulin-resistant HepG2 cells. As a result, compounds **1**, **3**, and **4** were found to significantly promote glucose consumption in the IR-HepG2 cells and therefore may hold potential as candidates for treating hyperglycemia.

EXPERIMENTAL SECTION

General Experimental Procedures. Optical rotations were determined in MeOH by using an Autopol IV polarimeter (Rudolph Research Analytical, Hackettstown, NJ, USA). UV spectra were recorded with a UH5300 UV−vis Double Beam spectrophotometer (Hitachi Co., Tokyo, Japan). 1D and 2D NMR spectra were recorded with a Bruker AVANCE IIITM 500 or 600 MHz spectrometer (Bruker, Ettlingen, Germany) in $CDCl_3$ using tetramethylsilane (TMS) as the internal standard. Chemical shifts (δ) are reported in ppm, and the coupling constants (J) are expressed in Hz. High-resolution electrospray mass spectroscopy (HR-ESI-MS) data were obtained using a Thermo Scientific Q Exactive Orbitrap LC−MS/MS System (Thermo Scientific, Waltham, MA, USA). High-performance liquid chromatography (HPLC) was conducted using an Ultimate 3000 HPLC system (Dionex Co., Sunnyvale, CA, USA). The system consisted of an Ultimate 3000 pump and Ultimate 3000 Variable Wavelength detector. A semipreparative YMC-Pack ODS-A column (250 × 10 mm, 5 mm) was utilized. Silica gel for column chromatography (CC) (200−300 mesh) was obtained from Qingdao Hai Yang Chemical Group Co. Ltd. (Qingdao, China). Acetonitrile of chromatographic grade was purchased from Chang Tech Enterprise Co., Ltd. (Taiwan, China). Dulbecco's modified Eagle medium (DMEM) and 0.25% pancreatin were purchased from Wuhan Procell Life Science Technology Co., Ltd. (Wuhan, China), and the glucose kit from Nanjing Jiancheng Bioengineering Institute (Nanjing, China). Metformin hydrochloride tablets were obtained from Sino-American Shanghai Squibb Pharmaceuticals Ltd. (Shanghai, China). Cell counting kit-8 (CCK-8) was purchased from ABclonal Technology Co., Ltd. (Wuhan, China). Glucose solution and palmitate acid (PA) were obtained from Sigma-Aldrich Co., Ltd. (St. Louis, MO, USA). Fetal bovine serum was purchased from Zhejiang Tianhang Biotechnology Co., Ltd. (Hangzhou, China).

Plant Material. The dried fruits of *G. bracteata* were collected from Jinping County, Honghe Prefecture, Yunnan Province, and identified by Prof. Hong Liu, College of Life Sciences, South-Central Minzu University. The voucher specimen (no. 2016120101) was deposited in the herbarium of the School of Pharmaceutical Sciences, South-Central Minzu University.

Extraction and Isolation. The air-dried fruits of *G. bracteata* (10.4 kg) were crushed and extracted using 95% ethanol (EtOH) three times at room temperature, with each time for 24 h. The combined 95% EtOH extract was evaporated in vacuo to give a light brown crude gum (2.6 kg). This crude gum was dissolved in water, and further extracted with ethyl acetate (EtOAc) three times, yielding 1.1 kg of EtOAc extract. The EtOAc extract was purified by silica gel CC with a petroleum ether (PE)-EtOAc gradient (9:1, 8:2, 7:3, 1:1, 3:7, and 0:1), resulting in the isolation of seven fractions (fractions A−G). Fraction E (128 g) was further purified through silica gel CC using PE-EtOAc (9:1, 8:2, 7:3, 1:1, 3:7, and 0:1) as the eluent, yielding six subfractions (fractions E−A−E−F). Fraction E−C was further purified through silica gel CC using a cyclohexane−EtOAc (30:1, 20:1, 10:1, 9:1, 8:2, and 0:1) as the eluent, yielding seven subfractions (fractions E-C.1−E-C.7). Fraction E-C.6 was subjected to repeated reversed phase silica gel CC and semipreparative HPLC to obtain compounds **1** (3.75 mg; t_R = 17.5 min; CH_3CN− H_2O containing 0.1% formic acid, 85:15, v/v) and **6** (1.13 mg; t_R = 12.8 min; CH_3CN−H_2O containing 0.1% formic acid, 78:22, v/v), respectively. Fraction E−D was further purified through silica CC using PE−EtOAc (9:1, 8:2, 7:3, 6:4, 4:6, 3:7, and 0:1) as the eluent, yielding six subfractions (fractions E-D.1−E-D.6). Fraction E-D.4 was subjected to repeated reversed phase silica gel CC and semipreparative HPLC to yield compounds **2** (5.02 mg; t_R = 96.6 min; CH_3CN−H_2O containing 0.1% formic acid, 51:49, v/v), **3** (9.10 mg; t_R = 38.3 min; CH_3CN−H_2O containing 0.1% formic acid, 50:50, v/v), **4** (18.46 mg; t_R = 40.1 min; CH_3CN−H_2O containing 0.1% formic acid, 50:50, v/v), **5** (0.10 mg; t_R = 31.2 min; CH_3CN−H_2O containing 0.1% formic acid, 66:34, v/v), respectively.

Garbractin A (1). White amorphous powder; $[\alpha]^{D}_{25}$ −94.4 (c 0.05, MeOH); UV (MeOH) λ_{max} (log ε): 210 (4.12), 315 (4.32) nm; ECD (9.05 × 10^{-4} M, MeOH) λ_{max} (θ) 212 (−3.10), 230 (−10.66), 279 (+0.40), 325 (−4.85) nm; ^{1}H NMR (500 MHz, $CDCl_3$) and ^{13}C NMR (125 MHz, $CDCl_3$): see Tables 1 and 2; HRESIMS m/z 553.3160 $[M + H]^+$ (calcd for $C_{33}H_{45}O_7$, 553.3160).

Garcibracteatone A (2). White amorphous powder; $[\alpha]^{D}_{22}$ +34.8 (c 0.25, MeOH); UV (MeOH) λ_{max} (log ε): 210 (3.95), 255 (3.97) nm; ECD (4.86 × 10^{-4} M, MeOH) λ_{max} (θ) 215 (+10.36), 233 (−0.02), 256 (+14.49), 281 (+0.99), 293 (+2.15), 325 (−6.53) nm; ^{1}H NMR (500 MHz, $CDCl_3$) and

^{13}C NMR (125 MHz, $CDCl_3$): see Tables 1 and 2; HRESIMS m/z 517.2952 $[M + H]^+$ (calcd for $C_{33}H_{41}O_5$, 517.2949).

Garcibracteatone B (3). White amorphous powder; $[\alpha]_{25}^{D}$ +8.08 (c 0.06, MeOH); UV (MeOH) λ_{max} (log ε): 210 (4.18), 255 (3.98) nm; ECD (1.02×10^{-3} M, MeOH) λ_{max} (θ) 215 (+11.15), 230 (−0.21), 255 (+18.24), 279 (+1.79), 294 (+3.00), 325 (−8.02) nm; ^{1}H NMR (600 MHz, $CDCl_3$) and ^{13}C NMR (150 MHz, $CDCl_3$): see Tables 1 and 2; HRESIMS m/z 557.2873 $[M + Na]^+$ (calcd for $C_{33}H_{42}O_6Na$, 557.2874).

Garcibracteatone C (4). Yellow powder; $[\alpha]_{25}^{D}$+ 46.18 (c 0.05, MeOH); UV (MeOH) λ_{max} (log ε): 210 (4.17), 255 (3.96) nm; ECD (9.60×10^{-4} M, MeOH) λ_{max} (θ) 215 (+10.92), 232 (+0.90), 256 (+15.80), 279 (+1.77), 294 (+2.98), 325 (−6.47) nm; ^{1}H NMR (600 MHz, $CDCl_3$) and ^{13}C NMR (150 MHz, $CDCl_3$): see Tables 1 and 2; HRESIMS m/z 535.3054 $[M + H]^+$ (calcd for $C_{33}H_{43}O_6$, 535.3054).

Garcibracteatone D (5). White amorphous powder; $[\alpha]_{25}^{D}$ −74.4 (c 0.01, MeOH); UV (MeOH) λ_{max} (log ε): 210 (4.37), 250 (4.21) nm; ECD (1.94×10^{-4} M, MeOH) λ_{max} (θ) 215 (+5.72), 230 (−2.82), 256 (+13.29), 279 (+1.10), 293 (+1.46), 324 (−5.86) nm; ^{1}H NMR (600 MHz, $CDCl_3$) and ^{13}C NMR (150 MHz, $CDCl_3$): see Tables 2 and 3; HRESIMS m/z 517.2951 $[M + H]^+$ (calcd for $C_{33}H_{41}O_5$, 517.2949).

Garcibracteatone E (6). White amorphous powder; $[\alpha]_{25}^{D}$ +3.63 (c 0.05, MeOH); UV (MeOH) λ_{max} (log ε): 210 (4.15), 250 (3.94) nm; ECD (9.49×10^{-4} M, MeOH) λ_{max} (θ) 216 (+8.91), 230 (−1.09), 255 (+13.45), 279 (+1.04), 292 (+1.45), 324 (−5.79) nm; ^{1}H NMR (500 MHz, $CDCl_3$) and ^{13}C NMR (125 MHz, $CDCl_3$): see Tables 1 and 2; HRESIMS m/z 539.2768 $[M + Na]^+$ (calcd for $C_{33}H_{40}O_5Na$, 539.2768).

NMR Calculations. Computational NMR data were derived from the IEFPCM model at the mPW1PW91/6-311+G (2d and p) level in methanol. The data were obtained by using the GIAO method. Detailed NMR calculations are provided in the Supporting Information.

ECD Calculations. ECD in methanol was derived from the IEFPCM model using time-dependent DFT (TD-DFT). Detailed ECD calculations are provided in the Supporting Information.

Determination of the Configurations of the Vic-Diols Units in Garcibracteatones B (3) and C (4). The absolute configuration of the *Vic*-diols unit in garcibracteatones B (**3**) and C (**4**) was determined using $Mo_2(OAc)_4$-induced ECD,[15,18] following the Snatzke rules. A stock solution of $Mo_2(OAc)_4$ (1.0 mg/mL) was prepared in anhydrous DMSO, and then, garcibracteatones B (0.9 mg) and C (0.9 mg) were added separately, maintaining a mass ratio of approximately 1.1:1. The $Mo_2(OAc)_4$-induced ECD was continuously recorded every 10 min until the IECD spectrum reached a nearly constant value. After subtracting the original ECD spectrum of garcibracteatones C and D, the presence of a Cotton effect around 310 nm indicated the configuration of C-25 in garcibracteatones C and D, as determined by the Snatzke rules.

Cell Viability. The viability of HepG2 cells was assayed by the CCK-8 method.[19]

Glucose Consumption in IR-HepG2 Cells. In this study, we conducted glucose consumption analysis following our previous research.[20] HepG2 cells (1.0×10^5 cells/well) were divided into four groups: normal control group (NC), PA-induced model group (MC), metformin hydrochloride (10 μM)-treated group (Met), and different doses of PPAP groups (5 and 10 μM or 2, 4, and 6 μM). All groups, except for the NC group, were cultured with 0.25 mM PA and 30 mM glucose to establish the IR model. Different concentrations of PPAPs or Met were added to the cells together with PA and glucose and incubated for 24 h. The concentration of glucose in the medium was determined using glucose assay kits (Nanjing Jiancheng Bioengineering Institute). To calculate glucose consumption, the glucose content of the original medium was subtracted from the glucose content of the medium in the cell-treated group. Each group was tested in six replicate wells, and the experiment was repeated three times.

■ ASSOCIATED CONTENT

Supporting Information

The Supporting Information is available free of charge at https://pubs.acs.org/doi/10.1021/acsomega.3c04947.

HRESIMS, UV, CD, and 1D and 2D NMR spectra of compounds 1−6; NMR calculations of compounds 1−2; ECD calculations of compounds 1−2; and RDC analysis of compound 1 (PDF)

■ AUTHOR INFORMATION

Corresponding Authors

Guang-Zhong Yang − *School of Pharmaceutical Sciences, South-Central Minzu University, Wuhan 430074, P. R. China; Ethnopharmacology Level 3 Laboratory, National Administration of Traditional Chinese Medicine, Wuhan 430074, P. R. China;* orcid.org/0000-0001-9853-5078; Email: yanggz888@126.com

Xin-Xiang Lei − *State Key Laboratory of Applied Organic Chemistry, College of Chemistry and Chemical Engineering, Lanzhou University, Lanzhou 73000, P. R. China;* orcid.org/0000-0002-5635-5375; Email: leixx@lzu.edu.cn

Yu Chen − *College of Chemistry and Material Sciences, South-Central Minzu University, Wuhan 430074, P. R. China;* Email: chenyuwh888@126.com

Authors

Xue-Ni Li − *School of Pharmaceutical Sciences, South-Central Minzu University, Wuhan 430074, P. R. China*

Jing Xu − *School of Pharmaceutical Sciences, South-Central Minzu University, Wuhan 430074, P. R. China*

Shuang Yang − *School of Pharmaceutical Sciences, South-Central Minzu University, Wuhan 430074, P. R. China*

Qing-Qing Li − *School of Pharmaceutical Sciences, South-Central Minzu University, Wuhan 430074, P. R. China*

Zheng-Yang Lu − *College of Chemistry and Material Sciences, South-Central Minzu University, Wuhan 430074, P. R. China*

Gui Mei − *School of Pharmaceutical Sciences, South-Central Minzu University, Wuhan 430074, P. R. China*

Jia-Qian Li − *School of Pharmaceutical Sciences, South-Central Minzu University, Wuhan 430074, P. R. China*

Complete contact information is available at: https://pubs.acs.org/10.1021/acsomega.3c04947

Author Contributions

[⊥]X.-N.L. and J.X. contributed equally.

Notes

The authors declare no competing financial interest.

■ ACKNOWLEDGMENTS

This work was supported by the National Key Research and Development Program (2022YFC3502200), Key Research and

Development Program of Hubei Province (2021ACB003), State Key Laboratory of Freshwater Ecology and Biotechnology (2022FB04), and Special Fund for Basic Scientific Research of Central Colleges, South-Central Minzu University (CZY22002).

■ REFERENCES

(1) (a) Yang, X. W.; Grossman, R. B.; Xu, G. Research Progress of Polycyclic Polyprenylated Acylphloroglucinols. *Chem. Rev.* **2018**, *118*, 3508−3558. (b) Ciochina, R.; Grossman, R. B. Polycyclic Polyprenylated Acylphloroglucinols. *Chem. Rev.* **2006**, *106*, 3963−3986. (c) Oya, A.; Tanaka, N.; Kusama, T.; Kim, S. Y.; Hayashi, S.; Kojoma, M.; Hishida, A.; Kawahara, N.; Sakai, K.; Gonoi, T.; Kobayashi, J. I. Prenylated Benzophenones from *Triadenum japonicum*. *J. Nat. Prod.* **2015**, *78*, 258−264.

(2) (a) Pepper, H. P.; Tulip, S. J.; Nakano, Y.; George, J. H. Biomimetic Total Synthesis of (±)-Doitunggarcinone A and (+)-Garcibracteatone. *J. Org. Chem.* **2014**, *79*, 2564−2573. (b) Pepper, H. P.; Lam, H. C.; Bloch, W. M.; George, J. H. Biomimetic Total Synthesis of (±)-Garcibracteatone. *Org. Lett.* **2012**, *14*, 5162−5164.

(3) (a) Chen, Y.; Gan, F.; Jin, S.; Liu, H.; Wu, S. J.; Yang, W. T.; Yang, G. Z. Adamantyl Derivatives and Rearranged Benzophenones from *Garcinia xanthochymus* Fruits. *RSC Adv.* **2017**, *7*, 17289−17296. (b) Chen, Y.; Xue, Q.; Teng, H. D.; Qin, R.; Liu, H.; Xu, J.; Mei, Z. N.; Yang, G. Z. Acylphloroglucinol Derivatives with a Tricyclo-[4.4.1.1^{1,4}] Dodecane Skeleton from *Garcinia bracteata* Fruits. *J. Org. Chem.* **2020**, *85*, 6620−6625. (c) Xue, Q.; Chen, Y.; Yin, H. J.; Teng, H. D.; Qin, R.; Liu, H.; Li, Q. Q.; Mei, Z. N.; Yang, G. Z. Prenylated Xanthones and Benzophenones from the Fruits of *Garcinia bracteata* and Their Potential Antiproliferative and Anti-inflammatory activities. *Bioorg. Chem.* **2020**, *104*, 104339.

(4) (a) Zheng, X. F.; Kadir, A.; Zheng, G. J.; Jin, P. F.; Qin, D. M.; Maiwulanjiang, M.; Aisa, H. A.; Yao, G. M. Antiproliferative Abietane Quinone Diterpenoids from the Roots of *Salvia deserta*. *Bioorg. Chem.* **2020**, *104*, 104261. (b) Zhan, G. Q.; Qu, X. L.; Liu, J. J.; Tong, Q. L.; Zhou, J. F.; Sun, B.; Yao, G. M. Zephycandidine A, the first Naturally Occurring Imidazo [1,2-f] Phenanthridine Alkaloid from *Zephyranthes candida*, Exhibits Significant Anti-tumor and Anti-acetylcholinesterase Activities. *Sci. Rep.* **2016**, *6*, 33990−33999.

(5) Costa, F. L. P.; de Albuquerque, A. C. F.; Fiorot, R. G.; Lião, L. M.; Martorano, L. H.; Mota, G. V. S.; Valverde, A. L.; Carneiro, J. W. M.; dos Santos Junior, F. M. Structural Characterisation of Natural Products by Means of Quantum Chemical Calculations of NMR Parameters: New Insights. *Org. Chem. Front.* **2021**, *8*, 2019−2058.

(6) Marcarino, M. O.; Cicetti, S.; Zanardi, M. M.; Sarotti, A. M. A Critical Review on the Use of DP4+ in the Structural Elucidation of Natural Products: the Good, the Bad and the Ugly. A Practical Guide. *Nat. Prod. Rep.* **2022**, *39*, 58−76.

(7) Wang, F. Q.; Sarotti, A. M.; Jiang, G. D.; Huguet-Tapia, J. C.; Zheng, S. L.; Wu, X. H.; Li, C. S.; Ding, Y. S.; Cao, S. G. Waikikiamides A−C: Complex Diketopiperazine Dimer and Diketopiperazine−polyketide Hybrids from a Hawaiian Marine Fungal Strain Aspergillus sp. FM242. *Org. Lett.* **2020**, *22*, 4408−4412.

(8) Lei, X.; Qiu, F.; Sun, H.; Bai, L.; Wang, W.-X.; Xiang, W.; Xiao, H. A Self-assembled Oligopeptide as a Versatile NMR Alignment Medium for the Measurement of Residual Dipolar Couplings in Methanol. *Angew. Chem., Int. Ed.* **2017**, *56*, 12857−12861.

(9) Enthart, A.; Freudenberger, J. C.; Furrer, J.; Kessler, H.; Luy, B. The CLIP/CLAP-HSQC: Pure Absorptive Spectra for the Measurement of One-bond Couplings. *J. Magn. Reson.* **2008**, *192*, 314−322.

(10) Navarro-Vázquez, A. MSpin-RDC. A Program for the Use of Residual Dipolar Couplings for Structure Elucidation of Small Molecules. *Magn. Reson. Chem.* **2012**, *50*, S73−S79.

(11) Thoison, O.; Cuong, D. D.; Gramain, A.; Chiaroni, A.; Hung, N. V.; Sévenet, T. Further Rearranged Prenylxanthones and Benzophenones from *Garcinia bracteata*. *Tetrahedron* **2005**, *61*, 8529−8535.

(12) Tantapakul, C.; Phakhodee, W.; Ritthiwigrom, T.; Cheenpracha, S.; Prawat, U.; Deachathai, S.; Laphookhieo, S. Rearranged Benzophenones and Prenylated Xanthones from *Garcinia propinqua twigs*. *J. Nat. Prod.* **2012**, *75*, 1660−1664.

(13) Shi, B. B.; Ai, H. L.; Duan, K. T.; Feng, T.; Liu, J. K. Ophiorrhines F and G, Key Biogenetic Intermediates of Ophiorrhine Alkaloids from *Ophiorrhiza japonica* and Their Immunosuppressant Activities. *J. Nat. Prod.* **2022**, *85*, 453−457.

(14) (a) Liao, Y.; Yang, S. Y.; Li, X. N.; Yang, X. W.; Xu, G. Polyprenylated Acylphloroglucinols from the Fruits of *Hypericum henryi*. *Sci. China: Chem.* **2016**, *59*, 1216−1223. (b) Zhang, J. J.; Yang, J.; Liao, Y.; Yang, X. W.; Ma, J. Z.; Xiao, Q. L.; Yang, L. X.; Xu, G. Hyperuralones A and B, New Acylphloroglucinol Derivatives with Intricately Caged Cores from *Hypericum uralum*. *Org. Lett.* **2014**, *16*, 4912−4915.

(15) (a) Di Bari, L.; Pescitelli, G.; Pratelli, C.; Pini, D.; Salvadori, P. Determination of Absolute Configuration of Acyclic 1, 2-diols with $Mo_2(OAc)_4$ Snatzke's Method Revisited. *J. Org. Chem.* **2001**, *66*, 4819−4825. (b) Liu, J.; Du, D.; Si, Y. K.; Lü, H. N.; Wu, X. F.; Li, Y.; Liu, Y. Y.; Yu, S. S. Application of Dimolybdenum Reagent $Mo_2(OAc)_4$ for Determination of the Absolute Configurations of vic-Diols. *Chin. J. Org. Chem.* **2010**, *30*, 1270−1278. (c) Zhang, H. Q.; Peng, X.; Zheng, X. F.; Li, S. Y.; Teng, Y.; Liu, J. J.; Zou, C. M.; Yao, G. M. Lanostane Triterpene Glycosides from the Flowers of *Lyonia ovalifolia* var. hebecarpa and Their Antiproliferative Activities. *Bioorg. Chem.* **2020**, *96*, 103598. (d) Ju, F.; Kuang, Q. X.; Li, Q. Z.; Huang, L. J.; Guo, W. X.; Gong, L. Q.; Dai, Y. F.; Wang, L.; Gu, Y. C.; Wang, D.; Deng, Y.; Guo, D. L. Aureonitol Analogues and Orsellinic Acid Esters Isolated from *Chaetomium elatum* and Their Antineuroinflammatory Activity. *J. Nat. Prod.* **2021**, *84*, 3044−3054.

(16) (a) Tian, W. J.; Qiu, Y. Q.; Jin, X. J.; Chen, H. F.; Yao, X. J.; Dai, Y.; Yao, X. S. Hypersampsones S−W, New Polycyclic Polyprenylated Acylphloroglucinols from *Hypericum sampsonii*. *RSC Adv.* **2016**, *6*, 50887−50894. (b) Jin, S.; Wang, W.; Gan, F.; Xie, W. L.; Xu, J.; Chen, Y.; Mei, Z. N.; Yang, G. Z. Discovery of Novel Polycyclic Polyprenylated Acylphloroglucinols from the Fruits of *Garcinia xanthochymus* as Antitumor Agents by Suppressing the STAT3 Signaling. *Int. J. Mol. Sci.* **2021**, *22*, 10365.

(17) Teng, H. D.; Li, Q. Q.; Ma, Z. Y.; Li, X. N.; Xie, W. L.; Chen, Y.; Yang, G. Z. Polyprenylated Acylphloroglucinols with Different Carbon Skeletons from the Fruits of *Garcinia multiflora*. *Front. Chem.* **2021**, *9*, 756452.

(18) Snatzke, G.; Wagner, U.; Wolff, H. P. Circulardichroism LXXV: Cottonogenic derivatives of chiral bidentate ligands with the complex $[Mo_2(O_2CCH_3)_4]$. *Tetrahedron* **1981**, *37*, 349−361.

(19) Li, Q. Q.; Xu, J.; Chen, Y. Y.; Xie, W. L.; Mei, G.; Li, X. N.; Chen, Y.; Yang, G. Z. Chemical Constituents from the Seeds of *Nigella glandulifera* and Their Hypoglycemic Activities. *RSC Adv.* **2022**, *12*, 19445−19451.

(20) Li, Q. Q.; Yang, S.; Teng, H. D.; Li, X. N.; Xie, W. L.; Wu, Z. L.; Yang, G. Z.; Xu, J.; Chen, Y. Structural Elucidation of Two Intricate Polycyclic Polyprenylated Acylphloroglucinols Using Quantum Chemical Calculations and Their Hypoglycemic Activities. *Arab. J. Chem.* **2022**, *15*, 104137.